



Power Flow Models of GaN Based Partial Parallel Dual Active Bridge (P2DAB) DC-DC Converter

Xiao, Yudi; Zhang, Zhe; Andersen, Michael A. E.

Published in:

Proceedings of 2nd IEEE International Power Electronics and Application Conference and Exposition

Link to article, DOI:

[10.1109/PEAC.2018.8590552](https://doi.org/10.1109/PEAC.2018.8590552)

Publication date:

2018

Document Version

Peer reviewed version

[Link back to DTU Orbit](#)

Citation (APA):

Xiao, Y., Zhang, Z., & Andersen, M. A. E. (2018). Power Flow Models of GaN Based Partial Parallel Dual Active Bridge (P2DAB) DC-DC Converter. In Proceedings of 2nd IEEE International Power Electronics and Application Conference and Exposition IEEE. DOI: 10.1109/PEAC.2018.8590552

General rights

Copyright and moral rights for the publications made accessible in the public portal are retained by the authors and/or other copyright owners and it is a condition of accessing publications that users recognise and abide by the legal requirements associated with these rights.

- Users may download and print one copy of any publication from the public portal for the purpose of private study or research.
- You may not further distribute the material or use it for any profit-making activity or commercial gain
- You may freely distribute the URL identifying the publication in the public portal

If you believe that this document breaches copyright please contact us providing details, and we will remove access to the work immediately and investigate your claim.

Power Flow Models of GaN Based Partial Parallel Dual Active Bridge (P2DAB) DC-DC Converter

Yudi Xiao
 Department of Electrical Engineering
 Technical University of Denmark
 Kgs. Lyngby, Denmark
 yudxiao@elektro.dtu.dk

Zhe Zhang
 Department of Electrical Engineering
 Technical University of Denmark
 Kgs. Lyngby, Denmark
 zz@elektro.dtu.dk

Michael A. E. Andersen
 Department of Electrical Engineering
 Technical University of Denmark
 Kgs. Lyngby, Denmark
 ma@elektro.dtu.dk

Abstract—This paper presents a lossless power flow model and an improved power flow model of the Partial Parallel Dual Active Bridge (P²DAB) dc-dc converter with single-phase-shift modulation (SPSM). The improved model considers the dead time and the parasitic elements. A GaN based P²DAB converter prototype is built to verify the models. The lossless model is more accurate than the other at small phase shift region, while the improved one is more accurate at medium and large phase shift region. The cause of the errors are discussed, and the solution to improve the accuracy is provided. Moreover, the improved model provides more details about the power flow characteristics than the lossless model.

Keywords—power flow model, dual active bridge converter, GaN

I. INTRODUCTION

Bidirectional converters, which can interface energy storage system (ESS) to power conversion systems, have gained increasing attention [1]-[3]. Due to its small number of components, symmetrical structure, isolation capability and soft switching properties, the dual active bridge (DAB) converter has become a popular topology [4] - [6].

In [7], a Partial Parallel Dual Active Bridge (P²DAB) converter, whose topology is shown in Fig. 1, is proposed. The basic idea of the structure is connecting the circuit parts, which need to carry high current, in parallel and connecting the circuit parts, which need to block high voltage, in series. The ac current balancing between the paralleled full-bridges (FBs) are inherently ensured by the winding series connection on the high-voltage (HV) side (V_1 side in Fig. 1). The basic control strategy of the P²DAB converter is single-phase-shift modulation (SPSM), i.e. add phase shift between the FB on the HV side (HVFB) and the FBs on the LV side (LVFB). In [7], in addition to the phase shift between the HVFB and the LVFBs, a phase shift is added between the LVFBs to increase the efficiency at the low power ranges. Power flow equations of the P²DAB converter are derived in [7]. However, these equations are ideal, neither losses nor dead time were considered. In [8], a lossless power flow model with consideration of dead time is derived for the DAB converter with SPSM. The effect of dead time on the power flow is addressed. In [9], a power flow model with consideration of both of the losses and the dead time is derived for the DAB converter with SPSM. And the power plateau and the anti-power phenomenon are discussed. These two phenomenon is addressed to have influences on the power flow control of the DAB converter with SPSM. Since the P²DAB converter is a DAB-based converter, it is thereby worthy to derive an improved power flow model for it with consideration of

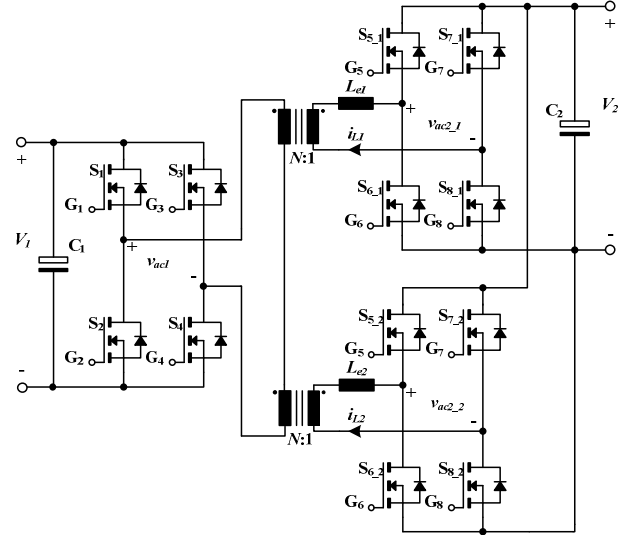


Fig. 1: Topology of the P²DAB converter

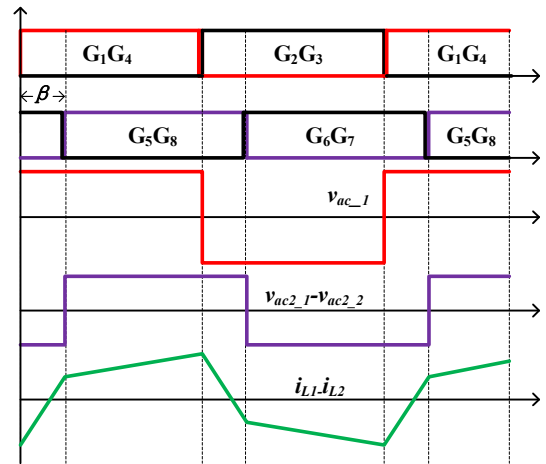


Fig. 2: Typical waveforms of the P²DAB converter with SPSM in lossless model, $V_1 \rightarrow V_2$, $V_1 > 2NV_2$

the losses and the dead time. With the improved model, the accurate prediction of the transferred power and the deep investigation of power flow characteristics of the P²DAB converter can be expected.

The paper is organized as follows: After this introduction, the modeling of the power flow of the P²DAB converter with SPSM is given in Section II. In Section III, both models are compared with the simulations. In Section IV, both models are compared with the experiments on a P²DAB converter prototype. Conclusions are made in Section V.

II. MODELLING OF THE P²DAB CONVERTER

A. Lossless Power Flow Model of the P²DAB Converter

In the lossless model, the following assumptions are made:

- The power semiconductor switches are ideal.
- Both transformers are ideal.
- Dead time is zero.

Typical waveforms of the P²DAB converter with SPSM under $V_1 \rightarrow V_2$ and $V_1 > 2NV_2$ are shown in Fig. 2. $V_1 \rightarrow V_2$ denotes the operation where power flows from V_1 to V_2 , and $V_2 \rightarrow V_1$ vice versa. β represents the electrical angle by which G_1 & G_4 (G_2 & G_3) leading G_5 & G_8 (G_6 & G_7), and β is also the phase difference between v_{ac1} and $v_{ac2,1}$ (or $v_{ac2,2}$) since the dead time is ignored in the lossless model. In [4], the lossless power flow model for the DAB converter with SPSM was derived. Using the same deriving procedures in [4], the lossless power flow model of the P²DAB converter with SPSM can be expressed by (1), where P_{in} is the averaged power sourcing from V_1 , P_o is the averaged power sinking into V_2 , f_s is the switching frequency, and L_e denotes the inductance of L_{e1} or L_{e2} . d is the unified phase shift angle, whose expression is given in (2).

$$P_{in} = P_o = \frac{V_1 V_2 (1 - |d|) d}{2 f_s L_e} \quad (1)$$

$$d = \frac{\beta}{\pi} \quad (2)$$

B. Improved Power Flow Model of the P²DAB Converter

Compared to the lossless model, the following circuit elements are considered in the improved model:

- The on-state resistances (R_{onH} , R_{onL}) and the free-wheeling voltage drops (V_{dH} , V_{dL}) of the switches.
- The leakage inductances (L_{trp} , L_{trs}) and the winding resistances (R_{trp} , R_{trs}) of the transformers.
- The winding resistances (R_e) of the external inductors.
- The dead time T_d .

Fig. 3 shows the derivation of the equivalent circuit of the P²DAB converter. In Fig. 3(a), the three FBs are firstly simplified to be three ac voltage sources, which are the voltages across the switching nodes of the three FBs, respectively. In Fig. 3(b), all the circuit elements on the LV side of the transformer are referred to the HV side. In Fig. 3(c), all the circuit elements in series are combined to further simplify the equivalent circuit. $v_{ac2,1}$ and $v_{ac2,2}$ are assumed to be the same, thereby both of them are represented by v_{ac2} . The expressions of L_{ac} and R_{ac} are given in (3).

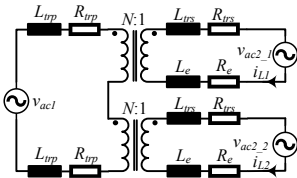


Fig. 3(a): Simplify the full-bridges

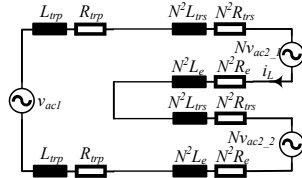


Fig. 3(b): Remove the transformer

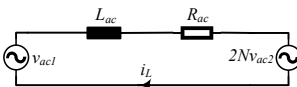


Fig. 3(c): Combine all the circuit elements in series

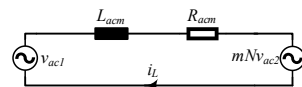


Fig. 4: Equivalent circuit of a P²DAB converter with multiple transformers

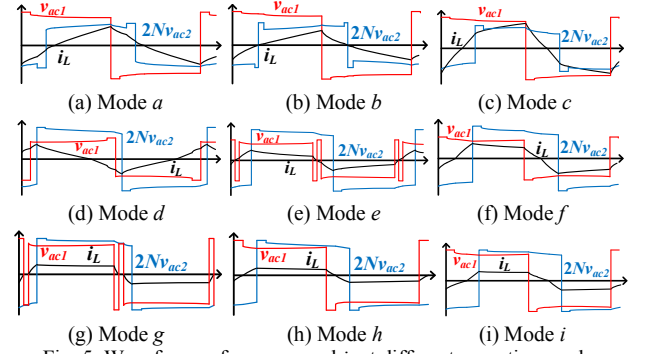


Fig. 5: Waveforms of v_{ac1} , v_{ac2} and i_L at different operation modes

$$L_{ac} = 2(L_{trp} + N^2 L_{trs} + N^2 L_e), R_{ac} = 2(R_{trp} + N^2 R_{trs} + N^2 R_e) \quad (3)$$

For a P²DAB converter with multiple transformers, where the number of branches is m , the equivalent circuit can be directly drawn as in Fig. 4. The expressions of L_{acm} and R_{acm} are given in (4). The model can also be applied to a DAB converter with SPSM by equaling m to 1.

$$L_{acm} = m(L_{trp} + N^2 L_{trs} + N^2 L_e), R_{acm} = m(R_{trp} + N^2 R_{trs} + N^2 R_e) \quad (4)$$

After deriving the equivalent circuit, the possible circuit operation modes need to be specified. The modes addressed in this paper for the P²DAB converter are the same as those determined in [8]. However, due to the consideration of the parasitic elements, the shape of the waveforms of v_{ac1} , $2Nv_{ac2}$ and i_L changes. Especially with the use of GaN devices, whose free-wheeling voltage drop is much larger than Silicon devices. Therefore, the waveforms of v_{ac1} , $2Nv_{ac2}$ and i_L at different operation modes need modifications. The modified waveforms for $V_1 \rightarrow V_2$ are given in Fig. 5. The operation conditions for Mode $a \sim$ Mode i in Fig. 5 are summarized in Table I. The waveforms for $V_2 \rightarrow V_1$ are of the same pattern as in Fig. 5, therefore are not given in this paper.

TABLE I: OPERATION CONDITIONS FOR DIFFERENT MODES

Mode	Operation Conditions
a	$V_1 > 2NV_2$, i_L changes direction after the dead time of the LVFB
b	$V_1 > 2NV_2$, i_L changes direction during the dead time of the LVFB
c	$V_1 > 2NV_2$, i_L changes direction before the dead time of the LVFB
d	$V_1 < 2NV_2$, i_L changes direction before the dead time of the HVFB
e	$V_1 < 2NV_2$, i_L changes direction during the dead time of the HVFB
f	$V_1 < 2NV_2$, i_L changes direction after the dead time of the HVFB
g	$V_1 \approx 2NV_2$, i_L decreases to zero during the dead time of the HVFB
h	$V_1 \approx 2NV_2$, i_L decreases to zero at the end of the dead time of the HVFB
i	$V_1 \approx 2NV_2$, i_L decreases to zero after the dead time of the HVFB

With the waveforms and the equivalent circuit, the improved power flow model of the P²DAB converter can be derived. Power flow equations of the P²DAB converter with SPSM in all of the 9 modes under both of the two power flow directions are given in the appendix.

III. SIMULATIONS

Fig. 6 depicts both the calculated power of the P²DAB converter by the lossless model and the simulated ones by Matlab with PLECS Blockset. Parameters used in the calculations and the simulations are given in Table II. As shown, the calculations and simulations are well matched. The derived lossless model is thereby valid.

TABLE II: PARAMETERS USED IN THE CALCULATIONS AND THE SIMULATIONS TO VERIFY THE LOSSLESS MODEL

V_1	600V	V_2	60V	N	4	f_s	300kHz
L_e	500nH	V_{dH}	3.8V	V_{dL}	2.5V	R_{onH}	65 m Ω
R_{onL}	3 m Ω	R_e	3 m Ω	R_{trp}	1.8 Ω	R_{trs}	80 m Ω
L_{tkp}	2.5uH	L_{lks}	110nH	T_d	120ns		

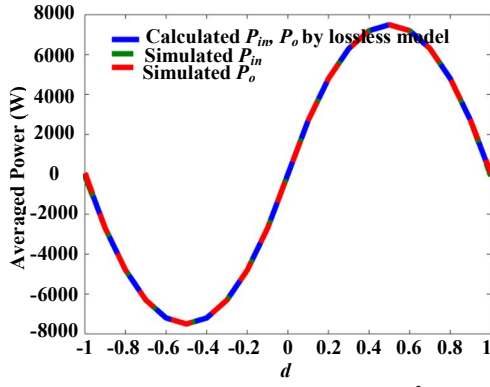


Fig. 6: Calculated power flow characteristics of the P²DAB converter by the lossless model and the corresponded simulations

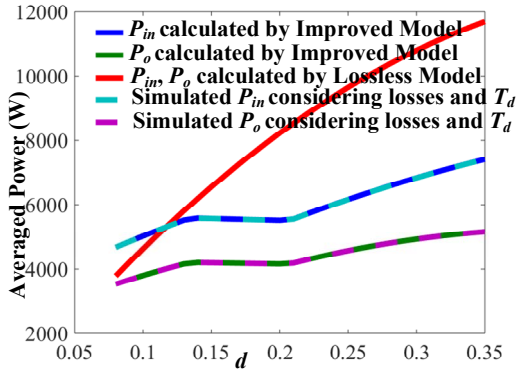


Fig. 7 (a) $V_1 \rightarrow V_2$, $V_1=600\text{V}$, $V_2=60\text{V}$, $N=7/3$

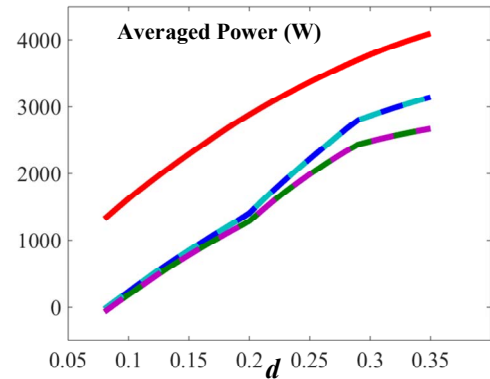


Fig. 7 (b) $V_1 \rightarrow V_2$, $V_1=600\text{V}$, $V_2=60\text{V}$, $N=20/3$

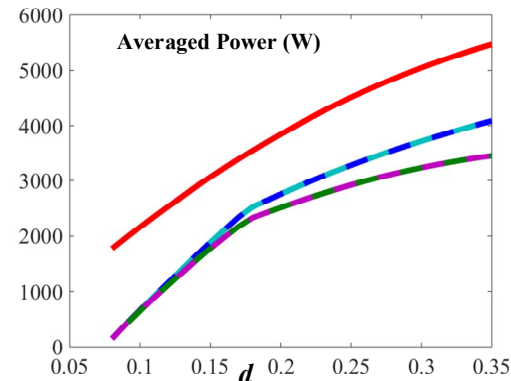


Fig. 7 (c) $V_1 \rightarrow V_2$, $V_1=601\text{V}$, $V_2=60\text{V}$, $N=15/3$

Fig. 7 gives both the calculated power of the P²DAB converter by the improved model and the simulated ones by Matlab with PLECS Blockset. The calculated power flow characteristics by the lossless model are also given in Fig. 7 for comparison.

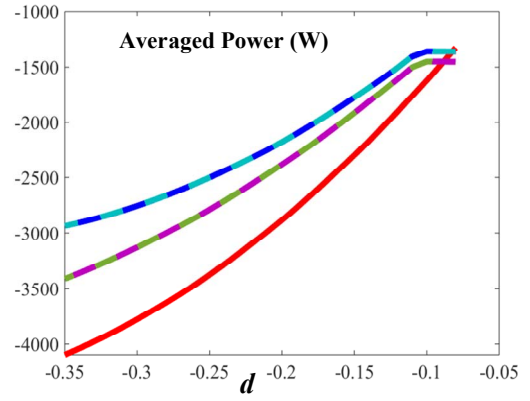


Fig. 7 (d) $V_2 \rightarrow V_1$, $V_1=600\text{V}$, $V_2=60\text{V}$, $N=20/3$

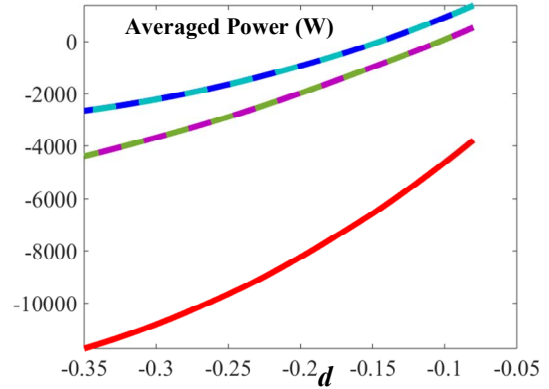


Fig. 7 (e) $V_2 \rightarrow V_1$, $V_1=600\text{V}$, $V_2=60\text{V}$, $N=7/3$

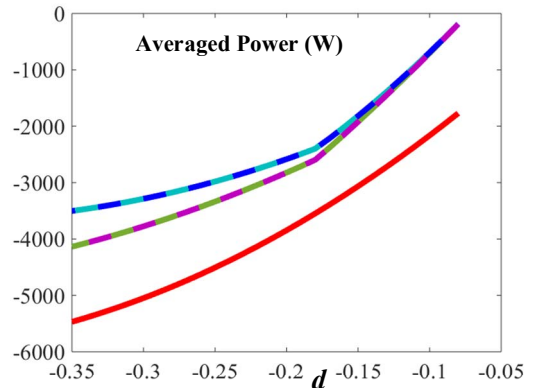


Fig. 7 (f) $V_2 \rightarrow V_1$, $V_1=601\text{V}$, $V_2=60\text{V}$, $N=15/3$

Fig. 7: Calculated power flow characteristics of the P²DAB converter by the improved model and the corresponded simulations

The absolute value of d in both calculations and simulations is limited to 0.35 because the phase shift angle is usually limited to small values (below $\pi/4$) to suppress the reactive losses in high-power applications. And a limited maximum d also helps reduce the simulation time.

As shown in Fig. 7, the calculated power by the improved model match the simulations well for all modes at both power flow directions. Therefore the improved power flow model is valid. Regarding the power flow characteristics, the improved model provides more details about the power flow than the lossless model. For this reason, the improved model is more suitable for investigating the power flow characteristics of the P²DAB converter.

IV. EXPERIMENTS

A GaN P²DAB prototype is built to investigate the accuracy of the two models. Key components used in the prototype are given in Table III. Fig. 9 shows a picture of the prototype. Fig. 10 compares the calculated P_{in} and P_o by both of the two models with the experimental results ($V_1=180V$, $V_2=15V$, $L_e=500nH$, $N=4$). As shown, both models have errors. The lossless model is more accurate at small d region, while the improved one is more accurate at medium and large d region. Moreover, the calculated power flow characteristics by the improved model shifted to the left down side of the tested power flow characteristics. The cause of this shift is the output capacitance of the switches. In the improved model, this capacitance is ignored, the rate of change of the switching node voltage during switching is considered to be infinite. However, as shown in Fig. 11, the experimental switching node voltage changes slowly during switching due to the output capacitance and the low-power operation. Therefore, the improved model shows low accuracy at the low power range. In order to obtain a high accuracy over the entire power range, the influence of the output capacitance of the switches need to be considered.

Also from Fig. 10, at specific d ranges, the tested averaged power decreases or nearly keeps unchanged when d increases. This so-called power plateau phenomenon addressed in [9] also exists in the P²DAB converter with SPSM, and it is only predicted by the improved model as shown in Fig. 7(a) and Fig. 7(d).

TABLE III: KEY COMPONENTS LIST

HV side GaN HEMT	GS66516B
LV side GaN HEMT	EPC2021
Transformer	ELP64/10/50, N97, PCB winding
Inductor	ELP43/10/28, N97, PCB winding

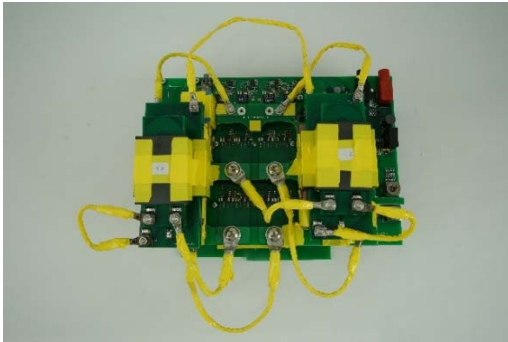


Fig. 9: P²DAB prototype

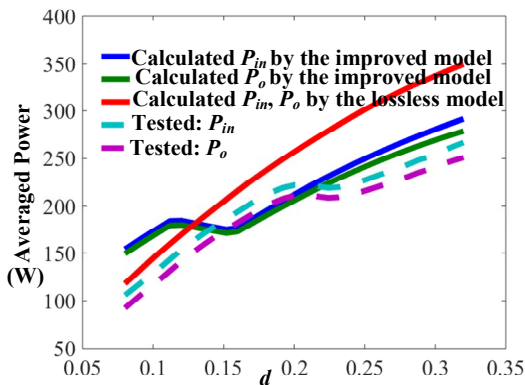


Fig. 10: Calculated and tested P_{in} and P_o

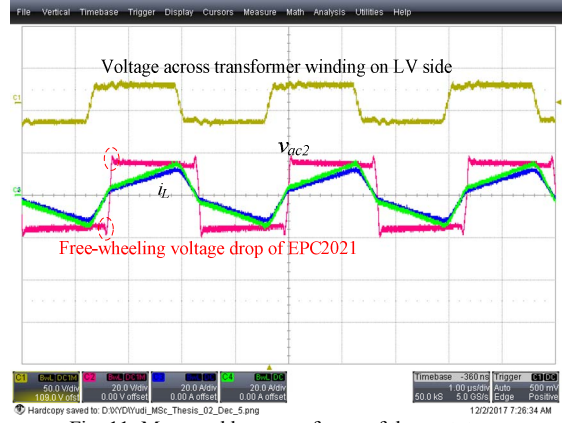


Fig. 11: Measured key waveforms of the prototype

IV. CONCLUSIONS AND FUTURE WORK

A lossless power flow model and an improved power flow model for the P²DAB converter with single-phase-shift modulation are derived. The improved model considers the dead time and the conduction losses of the switches and the magnetic components. Both models are compared with the experimental results. The lossless model is more accurate at small phase shift region, while the improved one is more accurate at medium and large phase shift region. In order to achieve high accuracy over the entire phase shift range, the output capacitance of the switches should be considered in the future work. And it is also proved that the improved model provides more details about the power flow characteristics of the P²DAB converter.

REFERENCES

- [1] B. Li, F. C. Lee, Q. Li, Z. Y. Liu, "Bi-directional on-board charger architecture and control for achieving ultra-high efficiency with wide battery voltage range," IEEE Applied Power Electronics Conference and Exposition (APEC), pp. 3688-3694, Mar. 2017.
- [2] R. M. Burkart, J. W. Kolar, "Comparative η - ρ - σ pareto optimization of Si and SiC multilevel Dual-Active-Bridge topologies with wide input voltage range," IEEE Trans. Power Electronics, vol. 32, no. 7, pp. 5258-5270, Jul. 2017.
- [3] F. Xue, R. Y. Yu, A. Q. Huang, "A 98.3% efficient GaN isolated bidirectional DC-DC converter for DC Microgrid energy storage system applications," IEEE Trans. Industrial Electronics, vol. 64, no. 11, pp. 9094-9103, Mar. 2017.
- [4] R. W. A. A. De Doncker, D. M. Divan, M. H. Kheraluwala, "A three-phase soft-switched high-power-density dc/dc converter for high-power applications," IEEE Trans. Industrial Applications, vol. 27, no. 1, pp. 63-73, Jan/Feb. 1991.
- [5] B. Zhao, Q. Song, J. G. Li, X. P. Xu, W. H. Liu, "Comparative analysis of multilevel-high-frequency-link and multilevel-dc-link DC-DC transformers based on MMC and Dual-Active bridge for MVDC application," IEEE Trans. Power Electronics, vol. 33, no. 3, pp. 2035-2049, Mar. 2018.
- [6] B. Zhao, Q. Song, J. G. Li, Q. H. Sun, W. H. Liu, "Full-process operation, control, and experiments of modular high-frequency-link DC transformer based on

dual active bridge for flexible MVDC distribution,” IEEE Trans. Power Electronics, vol. 32, no. 9, pp. 6751-6766, Sept. 2017.

[7] Z. Zhang, K. Tomas-Manez, Y. D. Xiao, M. A. E. Andersen, “High voltage gain dual active bridge converter with an extended operation range for renewable energy systems”, IEEE Applied Power Electronics Conference and Exposition (APEC), Mar. 2018.

[8] B. Zhao, Q. Song, W. H. Liu, Y. D. Sun, “Dead time effect of the high frequency isolated bidirectional full bridge dc-dc converter: comprehensive theoretical analysis and experimental verification”, IEEE Transactions on Power Electronics, vol. 29, No. 4, 2014: 1667-1680.

[9] Y. D. Xiao, Z. Zhang, K. Tomas-Manez, M. A. E. Andersen, “Power Plateau and Anti-Power Phenomenon of Dual Active Bridge Converter with Phase-Shift Modulation”, IEEE Applied Power Electronics Conference and Exposition (APEC), Mar. 2018.

APPENDIX

The following are the power flow equations of the improved model for the P²DAB converter with SPSM. Since the equations of current integrations are of the same form for all of the operation conditions, they are only given once as in (3).

(3) $V_1 \rightarrow V_2$, Mode a:

$$\begin{aligned} & \text{Condition: } V_1 > 2NV_2 \wedge d > 2T_d f_s \wedge i_L(t_{p1}) \geq 0 \\ & P_{in} = 2V_1 f_s (Int_1 + Int_2 + Int_3 + Int_4 + Int_5) \\ & P_o = 2V_2 \cdot 2Nf_s (Int_1 + Int_2 + Int_3 + Int_4 + Int_5) \\ & \Delta t_1 = T_d, \Delta t_2 = \frac{d}{2f_s} - T_d, \Delta t_3 = T_d, \Delta t_4 = \frac{1}{2f_s} \left(\frac{d}{2f_s} - T_d \right) \\ & \Delta t_5 = \frac{1}{2f_s} \left(\frac{d}{2f_s} - T_d \right) \\ & \Delta t_6 = \frac{1}{J_{p1}} \ln \left(\frac{M_{p1} + M_{p2} e^{-J_{p1} \Delta t_1} + M_{p3} e^{-J_{p1} \Delta t_2} + M_{p4} e^{-J_{p1} \Delta t_3} + M_{p5} e^{-J_{p1} \Delta t_4} + M_{p6} e^{-J_{p1} \Delta t_5}}{M_{p1} + M_{p2} + M_{p3} + M_{p4} + M_{p5} + M_{p6}} \right) \\ & J_{p1} = \frac{R_{ac} + 4N^2 R_{ont}}{L_{ac}}, J_{p2} = \frac{R_{ac} + 2R_{ont} + 4N^2 R_{ont}}{L_{ac}}, J_{p3} = \frac{R_{ac} + 2R_{ont}}{L_{ac}}, J_{p4} = \frac{R_{ac} + 2R_{ont} + 4N^2 R_{ont}}{L_{ac}}, J_{p5} = \frac{R_{ac} + 2R_{ont} + 4N^2 R_{ont}}{L_{ac}} \\ & M_{p1} = \frac{V_1 + 2V_{d1} + 2NV_2}{R_{ac} + 4N^2 R_{ont}}, M_{p2} = \frac{V_1 + 2NV_2}{R_{ac} + 2R_{ont} + 4N^2 R_{ont}}, M_{p3} = \frac{V_1 + 2N(V_2 + 2V_{d1})}{R_{ac} + 2R_{ont}}, M_{p4} = \frac{V_1 - 2NV_2}{R_{ac} + 2R_{ont} + 4N^2 R_{ont}}, M_{p5} = \frac{V_1 - 2NV_2}{R_{ac} + 2R_{ont} + 4N^2 R_{ont}} \end{aligned}$$

(4) $V_1 \rightarrow V_2$, Mode b:

$$\begin{aligned} & \text{Condition: } V_1 > 2NV_2 \wedge d > 2T_d f_s \wedge i_L(t_{p2}) < 0 \wedge i_L(t_{p4}) > 0 \\ & P_{in} = 2V_1 f_s (Int_{p1} + Int_{p2} + Int_{p3} + Int_{p4} + Int_{p5}) \\ & P_o = 2V_2 \cdot 2Nf_s (-Int_{p1} - Int_{p2} - Int_{p3} + Int_{p4} + Int_{p5}) \\ & \Delta t_{p1} = T_d, \Delta t_{p2} = \frac{d}{2f_s} - T_d, \Delta t_{p3} = T_d, \Delta t_{p4} = \frac{1}{2f_s} - \Delta t_{p1} - \Delta t_{p2} - \Delta t_{p3} - \Delta t_{p4} \\ & \Delta t_{p5} = \frac{1}{J_{p1}} \ln \left(\frac{M_{p1} + M_{p2} e^{-J_{p1} \Delta t_{p1}} + M_{p3} e^{-J_{p1} \Delta t_{p2}} + M_{p4} e^{-J_{p1} \Delta t_{p3}} + M_{p5} e^{-J_{p1} \Delta t_{p4}} + M_{p6} e^{-J_{p1} \Delta t_{p5}}}{M_{p1} + M_{p2} + M_{p3} + M_{p4} + M_{p5} + M_{p6}} \right) \\ & J_{p1} = \frac{R_{ac} + 4N^2 R_{ont}}{L_{ac}}, J_{p2} = \frac{R_{ac} + 2R_{ont} + 4N^2 R_{ont}}{L_{ac}}, J_{p3} = \frac{R_{ac} + 2R_{ont}}{L_{ac}}, J_{p4} = \frac{R_{ac} + 2R_{ont} + 4N^2 R_{ont}}{L_{ac}}, J_{p5} = \frac{R_{ac} + 2R_{ont} + 4N^2 R_{ont}}{L_{ac}} \\ & M_{p1} = \frac{V_1 + 2V_{d1} + 2NV_2}{R_{ac} + 4N^2 R_{ont}}, M_{p2} = \frac{V_1 + 2NV_2}{R_{ac} + 2R_{ont} + 4N^2 R_{ont}}, M_{p3} = \frac{V_1 + 2N(V_2 + 2V_{d1})}{R_{ac} + 2R_{ont}}, M_{p4} = \frac{V_1 - 2NV_2}{R_{ac} + 2R_{ont} + 4N^2 R_{ont}}, M_{p5} = \frac{V_1 - 2NV_2}{R_{ac} + 2R_{ont} + 4N^2 R_{ont}} \end{aligned}$$

(5) $V_1 \rightarrow V_2$, Mode c:

$$\begin{aligned} & \text{Condition: } V_1 > 2NV_2 \wedge d > 2T_d f_s \wedge i_L(t_{p3}) \geq 0 \\ & P_{in} = 2V_1 f_s (Int_{p1} + Int_{p2} + Int_{p3} + Int_{p4} + Int_{p5}) \\ & P_o = 2V_2 \cdot 2Nf_s (-Int_{p1} - Int_{p2} - Int_{p3} + Int_{p4} + Int_{p5}) \\ & \Delta t_{p1} = T_d, \Delta t_{p2} = \frac{d}{2f_s} - T_d, \Delta t_{p3} = T_d, \Delta t_{p4} = \frac{1}{2f_s} - T_d, \Delta t_{p5} = T_d \\ & \Delta t_{p6} = \frac{1}{J_{p1}} \ln \left(\frac{M_{p1} + M_{p2} e^{-J_{p1} \Delta t_{p1}} + M_{p3} e^{-J_{p1} \Delta t_{p2}} + M_{p4} e^{-J_{p1} \Delta t_{p3}} + M_{p5} e^{-J_{p1} \Delta t_{p4}} + M_{p6} e^{-J_{p1} \Delta t_{p5}}}{M_{p1} + M_{p2} + M_{p3} + M_{p4} + M_{p5} + M_{p6}} \right) \\ & J_{p1} = \frac{R_{ac} + 4N^2 R_{ont}}{L_{ac}}, J_{p2} = \frac{R_{ac} + 2R_{ont} + 4N^2 R_{ont}}{L_{ac}}, J_{p3} = \frac{R_{ac} + 2R_{ont}}{L_{ac}}, J_{p4} = \frac{R_{ac} + 2R_{ont} + 4N^2 R_{ont}}{L_{ac}}, J_{p5} = \frac{R_{ac} + 2R_{ont} + 4N^2 R_{ont}}{L_{ac}} \\ & M_{p1} = \frac{V_1 + 2V_{d1} + 2NV_2}{R_{ac} + 4N^2 R_{ont}}, M_{p2} = \frac{V_1 + 2NV_2}{R_{ac} + 2R_{ont} + 4N^2 R_{ont}}, M_{p3} = \frac{V_1 + 2N(V_2 + 2V_{d1})}{R_{ac} + 2R_{ont}}, M_{p4} = \frac{V_1 - 2NV_2}{R_{ac} + 2R_{ont} + 4N^2 R_{ont}}, M_{p5} = \frac{V_1 - 2NV_2}{R_{ac} + 2R_{ont} + 4N^2 R_{ont}} \end{aligned}$$

(6) $V_1 \rightarrow V_2$, Mode d:

$$\begin{aligned} & \text{Condition: } V_1 < 2NV_2 \wedge d > 2T_d f_s \wedge i_L(t_{p10}) \geq 0 \\ & P_{in} = 2V_1 f_s (-Int_{p1} + Int_{p2} + Int_{p3} + Int_{p4} + Int_{p5}) \\ & P_o = 2V_2 \cdot 2Nf_s (-Int_{p1} + Int_{p2} + Int_{p3} + Int_{p4} + Int_{p5}) \\ & \Delta t_{p1} = T_d, \Delta t_{p2} = \frac{d}{2f_s} - T_d, \Delta t_{p3} = T_d, \Delta t_{p4} = \frac{1}{2f_s} - T_d, \Delta t_{p5} = T_d \\ & \Delta t_{p6} = \frac{1}{J_{p1}} \ln \left(\frac{M_{p1} + M_{p2} e^{-J_{p1} \Delta t_{p1}} + M_{p3} e^{-J_{p1} \Delta t_{p2}} + M_{p4} e^{-J_{p1} \Delta t_{p3}} + M_{p5} e^{-J_{p1} \Delta t_{p4}} + M_{p6} e^{-J_{p1} \Delta t_{p5}}}{M_{p1} + M_{p2} + M_{p3} + M_{p4} + M_{p5} + M_{p6}} \right) \\ & J_{p1} = \frac{R_{ac} + 4N^2 R_{ont}}{L_{ac}}, J_{p2} = \frac{R_{ac} + 2R_{ont} + 4N^2 R_{ont}}{L_{ac}}, J_{p3} = \frac{R_{ac} + 2R_{ont}}{L_{ac}}, J_{p4} = \frac{R_{ac} + 2R_{ont} + 4N^2 R_{ont}}{L_{ac}}, J_{p5} = \frac{R_{ac} + 2R_{ont} + 4N^2 R_{ont}}{L_{ac}} \\ & M_{p1} = \frac{V_1 + 2V_{d1} + 2NV_2}{R_{ac} + 4N^2 R_{ont}}, M_{p2} = \frac{V_1 + 2NV_2}{R_{ac} + 2R_{ont} + 4N^2 R_{ont}}, M_{p3} = \frac{V_1 + 2N(V_2 + 2V_{d1})}{R_{ac} + 2R_{ont}}, M_{p4} = \frac{V_1 - 2NV_2}{R_{ac} + 2R_{ont} + 4N^2 R_{ont}}, M_{p5} = \frac{V_1 - 2NV_2}{R_{ac} + 2R_{ont} + 4N^2 R_{ont}} \end{aligned}$$

(7) $V_1 \rightarrow V_2$, Mode e:

$$\begin{aligned} & \text{Condition: } V_1 < 2NV_2 \wedge d > 2T_d f_s \wedge i_L(t_{p60}) < 0 \wedge i_L(t_{p2}) > 0 \\ & P_{in} = 2V_1 f_s (Int_{p1} - Int_{p2} + Int_{p3} + Int_{p4} + Int_{p5}) \\ & P_o = 2V_2 \cdot 2Nf_s (-Int_{p1} - Int_{p2} - Int_{p3} + Int_{p4} + Int_{p5}) \\ & \Delta t_{p1} = T_d, \Delta t_{p2} = \frac{d}{2f_s} - T_d, \Delta t_{p3} = T_d, \Delta t_{p4} = T_d, \Delta t_{p5} = \frac{1}{2f_s} - T_d \\ & \Delta t_{p6} = \frac{1}{J_{p1}} \ln \left(\frac{M_{p1} + M_{p2} e^{-J_{p1} \Delta t_{p1}} + M_{p3} e^{-J_{p1} \Delta t_{p2}} + M_{p4} e^{-J_{p1} \Delta t_{p3}} + M_{p5} e^{-J_{p1} \Delta t_{p4}} + M_{p6} e^{-J_{p1} \Delta t_{p5}}}{M_{p1} + M_{p2} + M_{p3} + M_{p4} + M_{p5} + M_{p6}} \right) \\ & J_{p1} = \frac{R_{ac} + 4N^2 R_{ont}}{L_{ac}}, J_{p2} = \frac{R_{ac} + 2R_{ont} + 4N^2 R_{ont}}{L_{ac}}, J_{p3} = \frac{R_{ac} + 2R_{ont}}{L_{ac}}, J_{p4} = \frac{R_{ac} + 2R_{ont} + 4N^2 R_{ont}}{L_{ac}}, J_{p5} = \frac{R_{ac} + 2R_{ont} + 4N^2 R_{ont}}{L_{ac}} \\ & M_{p1} = \frac{V_1 + 2V_{d1} + 2NV_2}{R_{ac} + 4N^2 R_{ont}}, M_{p2} = \frac{V_1 + 2NV_2}{R_{ac} + 2R_{ont} + 4N^2 R_{ont}}, M_{p3} = \frac{V_1 + 2N(V_2 + 2V_{d1})}{R_{ac} + 2R_{ont}}, M_{p4} = \frac{V_1 - 2NV_2}{R_{ac} + 2R_{ont} + 4N^2 R_{ont}}, M_{p5} = \frac{V_1 - 2NV_2}{R_{ac} + 2R_{ont} + 4N^2 R_{ont}} \end{aligned}$$

(8) $V_1 \rightarrow V_2$, Mode f:

$$\begin{aligned} & \text{Condition: } V_1 < 2NV_2 \wedge d > 2T_d f_s \wedge i_L(t_{p1}) \leq 0 \\ & P_{in} = 2V_1 f_s (Int_{p1} + Int_{p2} + Int_{p3} + Int_{p4} + Int_{p5}) \\ & P_o = 2V_2 \cdot 2Nf_s (-Int_{p1} - Int_{p2} - Int_{p3} + Int_{p4} + Int_{p5}) \\ & \Delta t_{p1} = T_d, \Delta t_{p2} = \frac{d}{2f_s} - T_d, \Delta t_{p3} = \frac{d}{2f_s} - T_d, \Delta t_{p4} = T_d, \Delta t_{p5} = \frac{1}{2f_s} - T_d \\ & \Delta t_{p6} = \frac{1}{J_{p1}} \ln \left(\frac{M_{p1} + M_{p2} e^{-J_{p1} \Delta t_{p1}} + M_{p3} e^{-J_{p1} \Delta t_{p2}} + M_{p4} e^{-J_{p1} \Delta t_{p3}} + M_{p5} e^{-J_{p1} \Delta t_{p4}} + M_{p6} e^{-J_{p1} \Delta t_{p5}}}{M_{p1} + M_{p2} + M_{p3} + M_{p4} + M_{p5} + M_{p6}} \right) \\ & J_{p1} = \frac{R_{ac} + 4N^2 R_{ont}}{L_{ac}}, J_{p2} = \frac{R_{ac} + 2R_{ont} + 4N^2 R_{ont}}{L_{ac}}, J_{p3} = \frac{R_{ac} + 2R_{ont}}{L_{ac}}, J_{p4} = \frac{R_{ac} + 2R_{ont} + 4N^2 R_{ont}}{L_{ac}}, J_{p5} = \frac{R_{ac} + 2R_{ont} + 4N^2 R_{ont}}{L_{ac}} \\ & M_{p1} = \frac{V_1 + 2V_{d1} + 2NV_2}{R_{ac} + 4N^2 R_{ont}}, M_{p2} = \frac{V_1 + 2NV_2}{R_{ac} + 2R_{ont} + 4N^2 R_{ont}}, M_{p3} = \frac{V_1 + 2N(V_2 + 2V_{d1})}{R_{ac} + 2R_{ont}}, M_{p4} = \frac{V_1 - 2NV_2}{R_{ac} + 2R_{ont} + 4N^2 R_{ont}}, M_{p5} = \frac{V_1 - 2NV_2}{R_{ac} + 2R_{ont} + 4N^2 R_{ont}} \end{aligned}$$

(9) $V_1 \rightarrow V_2$, Mode g:

$$\left\{ \begin{array}{l} \text{Condition : } V_1 \approx 2NV_2 \wedge d > 2T_d f_s, d < \frac{2f_s}{J_{p84}} \cdot \ln \left(\frac{-M_{p82} e^{-J_{p83} M_{p83} + J_{p82} T_d - J_{p84} \left(\frac{1}{2f_s} T_d\right)} + M_{p84} + i_L(t_{p80})}{(M_{p83} - M_{p84} + (M_{p82} - M_{p83}) e^{-J_{p83} M_{p83}}) e^{-J_{p84} \left(\frac{1}{2f_s} T_d\right)}} \right) \\ P_{in} = 2V_1 f_s (Int_{p81} + Int_{p83} + Int_{p84} + Int_{p85}) \\ P_o = 2V_2 \cdot 2Nf_s (-Int_{p81} - Int_{p83} + Int_{p84} + Int_{p85}) \\ \Delta t_{p85} = \frac{1}{2f_s} \cdot \frac{d}{2f_s} - T_d, \Delta t_{p82} = T_d - \Delta t_{p81}, \Delta t_{p83} = \frac{d}{2f_s} - T_d, \Delta t_{p84} = T_d, \\ \Delta t_{p81} = \left(-\frac{1}{J_{p81}} \right) \cdot \ln \left(\frac{M_{p81}}{M_{p81} + M_{p83} (1 - e^{-J_{p83} M_{p83}}) e^{-J_{p84} M_{p84} + J_{p83} M_{p83}}} \right. \\ \left. + M_{p82} e^{-J_{p83} M_{p83}} (1 - e^{-J_{p83} M_{p83}}) + M_{p83} (1 - e^{-J_{p83} M_{p83}}) \right) \\ J_{p81} = \frac{R_{ac} + 4N^2 R_{ont}}{L_{ac}}, J_{p82} = \text{Not Exist}, J_{p83} = \frac{R_{ac} + 2R_{ont} + 4N^2 R_{ont}}{L_{ac}} \\ J_{p84} = \frac{R_{ac} + 2R_{ont}}{L_{ac}}, J_{p85} = \frac{R_{ac} + 2R_{ont} + 4N^2 R_{ont}}{L_{ac}}, M_{p81} = \frac{V_1 + 2V_{dH} + 2NV_2}{R_{ac} + 4N^2 R_{ont}} \\ M_{p82} = \text{Not Exist}, M_{p83} = \frac{V_1 + 2NV_2}{R_{ac} + 2R_{ont} + 4N^2 R_{ont}}, M_{p84} = \frac{V_1 - 2N(V_2 + 2V_{dH})}{R_{ac} + 2R_{ont}}, M_{p85} = \frac{V_1 - 2NV_2}{R_{ac} + 2R_{ont} + 4N^2 R_{ont}} \end{array} \right.$$

(10) $V_I \rightarrow V_2$, Mode h :

$$\left\{ \begin{array}{l} \text{Condition : } V_1 \approx 2NV_2 \wedge d > 2T_d f_s, d = \frac{2f_s}{J_{p84}} \cdot \ln \left(\frac{-M_{p82} e^{-J_{p83} M_{p83} + J_{p82} T_d - J_{p84} \left(\frac{1}{2f_s} T_d\right)} + M_{p84} + i_L(t_{p80})}{(M_{p83} - M_{p84} + (M_{p82} - M_{p83}) e^{-J_{p83} M_{p83}}) e^{-J_{p84} \left(\frac{1}{2f_s} T_d\right)}} \right) \\ P_{in} = 2V_1 f_s (Int_{p81} + Int_{p82} + Int_{p83} + Int_{p84}) \\ P_o = 2V_2 \cdot 2Nf_s (-Int_{p81} - Int_{p82} + Int_{p83} + Int_{p84}) \\ \Delta t_{p81} = T_d, \Delta t_{p82} = \frac{d}{2f_s} - T_d, \Delta t_{p83} = T_d, \Delta t_{p84} = \frac{1}{2f_s} \cdot \frac{d}{2f_s} - T_d, \Delta t_{p85} = 0 \\ J_{p81} = \frac{R_{ac} + 4N^2 R_{ont}}{L_{ac}}, J_{p82} = \frac{R_{ac} + 2R_{ont} + 4N^2 R_{ont}}{L_{ac}}, J_{p83} = \frac{R_{ac} + 2R_{ont}}{L_{ac}} \\ J_{p84} = \frac{R_{ac} + 2R_{ont} + 4N^2 R_{ont}}{L_{ac}}, J_{p85} = \text{Not Exist} \\ M_{p81} = \frac{V_1 + 2V_{dH} + 2NV_2}{R_{ac} + 4N^2 R_{ont}}, M_{p82} = \frac{V_1 + 2NV_2}{R_{ac} + 2R_{ont} + 4N^2 R_{ont}}, M_{p83} = \frac{V_1 - 2N(V_2 + 2V_{dH})}{R_{ac} + 2R_{ont}} \\ M_{p84} = \frac{V_1 - 2NV_2}{R_{ac} + 2R_{ont} + 4N^2 R_{ont}}, M_{p85} = \text{Not Exist} \end{array} \right.$$

(11) $V_I \rightarrow V_2$, Mode i :

$$\left\{ \begin{array}{l} \text{Condition : } V_1 \approx 2NV_2, d > \frac{2f_s}{J_{p84}} \cdot \ln \left(\frac{-M_{p82} e^{-J_{p83} M_{p83} + J_{p82} T_d - J_{p84} \left(\frac{1}{2f_s} T_d\right)} + M_{p84} + i_L(t_{p80})}{(M_{p83} - M_{p84} + (M_{p82} - M_{p83}) e^{-J_{p83} M_{p83}}) e^{-J_{p84} \left(\frac{1}{2f_s} T_d\right)}} \right) \\ P_{in} = -2V_1 f_s (-Int_{p81} - Int_{p82} - Int_{p83} + Int_{p84} + Int_{p85}) \\ P_o = -2V_2 \cdot 2Nf_s (Int_{p81} + Int_{p82} + Int_{p83} + Int_{p84} + Int_{p85}) \\ \Delta t_{p81} = T_d, \Delta t_{p82} = \frac{d}{2f_s} - T_d, \Delta t_{p83} = T_d, \Delta t_{p84} = T_d, \Delta t_{p85} = \frac{1}{2f_s} \cdot \frac{d}{2f_s} - T_d \\ \Delta t_{p81} = \left(-\frac{1}{J_{p81}} \right) \cdot \ln \left(\frac{M_{p82} + M_{p83} e^{-J_{p83} M_{p83} + J_{p82} M_{p82} + J_{p81} \left(\frac{d}{2f_s} T_d\right)}}{M_{p82} + M_{p83} e^{-J_{p83} M_{p83} + J_{p82} M_{p82} + J_{p81} \left(\frac{d}{2f_s} T_d\right)} + M_{p84} (1 - e^{-J_{p84} M_{p84}}) e^{-J_{p84} \left(\frac{1}{2f_s} T_d\right)}} \right. \\ \left. + M_{p85} (1 - e^{-J_{p85} M_{p85}}) e^{-J_{p85} M_{p85}} - M_{p81} (1 - e^{-J_{p81} M_{p81}}) \right) \\ J_{p81} = \frac{R_{ac} + 4N^2 R_{ont}}{L_{ac}}, J_{p82} = \frac{R_{ac} + 2R_{ont} + 4N^2 R_{ont}}{L_{ac}}, J_{p83} = \frac{R_{ac} + 2R_{ont} + 4N^2 R_{ont}}{L_{ac}} \\ J_{p84} = \frac{R_{ac} + 2R_{ont}}{L_{ac}}, J_{p85} = \frac{R_{ac} + 2R_{ont} + 4N^2 R_{ont}}{L_{ac}}, M_{p81} = \frac{V_1 + 2V_{dH} + 2NV_2}{R_{ac} + 4N^2 R_{ont}} \\ M_{p82} = \frac{V_1 + 2NV_2}{R_{ac} + 2R_{ont} + 4N^2 R_{ont}}, M_{p83} = \frac{V_1 - 2N(V_2 + 2V_{dH})}{R_{ac} + 2R_{ont}}, M_{p84} = \frac{V_1 - 2NV_2}{R_{ac} + 2R_{ont} + 4N^2 R_{ont}} \\ M_{p85} = \frac{V_1 - 2NV_2}{R_{ac} + 2R_{ont} + 4N^2 R_{ont}} \end{array} \right.$$

(12) $V_2 \rightarrow V_I$, Mode a :

$$\left\{ \begin{array}{l} \text{Condition : } 2NV_2 > V_1 \wedge -d > 2T_d f_s \wedge i_L(t_{N33}) \leq 0 \\ P_{in} = -2V_2 \cdot 2Nf_s (Int_{p91} + Int_{p92} + Int_{p93} + Int_{p94} + Int_{p95}) \\ P_o = -2V_1 f_s (-Int_{p91} - Int_{p92} - Int_{p93} + Int_{p94} + Int_{p95}) \\ \Delta t_{n91} = T_d, \Delta t_{n92} = \frac{d}{2f_s} - T_d, \Delta t_{n93} = T_d, \Delta t_{n94} = \frac{1}{2f_s} \cdot \frac{d}{2f_s} - T_d - \Delta t_{N35} \\ \Delta t_{n91} = \left(-\frac{1}{J_{N35}} \right) \cdot \ln \left(\frac{\left((M_{N34} - M_{N33}) e^{J_{N32} M_{N32} + J_{N31} M_{N31}} + (M_{N33} - M_{N32}) e^{J_{N32} M_{N32}} \right)}{M_{N35} e^{-J_{N31} M_{N31}} + M_{N34} e^{J_{N32} M_{N32} + J_{N31} M_{N31} + J_{N34} \left(\frac{1}{2f_s} T_d - \frac{d}{2f_s} T_d\right)}} \right) \\ J_{n91} = \frac{R_{ac} + 2R_{ont}}{L_{ac}}, J_{n92} = \frac{R_{ac} + 2R_{ont} + 4N^2 R_{ont}}{L_{ac}}, J_{n93} = \frac{R_{ac} + 4N^2 R_{ont}}{L_{ac}}, J_{n94} = \frac{R_{ac} + 2R_{ont} + 4N^2 R_{ont}}{L_{ac}} \\ J_{n95} = \frac{R_{ac} + 2R_{ont} + 4N^2 R_{ont}}{L_{ac}}, M_{n91} = \frac{V_1 + 2N(V_2 + 2V_{dH})}{R_{ac} + 2R_{ont}}, M_{n92} = \frac{V_1 + 2NV_2}{R_{ac} + 2R_{ont} + 4N^2 R_{ont}} \\ M_{n93} = \frac{V_1 + 2V_{dH} + 2NV_2}{R_{ac} + 4N^2 R_{ont}}, M_{n94} = \frac{2NV_2 - V_1}{R_{ac} + 2R_{ont}}, M_{n95} = \frac{2NV_2 - V_1}{R_{ac} + 2R_{ont} + 4N^2 R_{ont}} \end{array} \right.$$

(13) $V_2 \rightarrow V_I$, Mode b :

$$\left\{ \begin{array}{l} \text{Condition : } 2NV_2 > V_1 \wedge -d > 2T_d f_s \wedge i_L(t_{N22}) < 0 \wedge i_L(t_{N24}) > 0 \\ P_{in} = -2V_1 f_s (-Int_{p91} - Int_{p92} - Int_{p93} + Int_{p94} + Int_{p95}) \\ P_o = -2V_2 \cdot 2Nf_s (Int_{p91} + Int_{p92} + Int_{p93} + Int_{p94} + Int_{p95}) \\ \Delta t_{n91} = T_d, \Delta t_{n92} = \frac{d}{2f_s} - T_d, \Delta t_{n93} = T_d - \Delta t_{N24}, \Delta t_{n95} = \frac{1}{2f_s} \cdot \frac{d}{2f_s} - T_d \\ \Delta t_{n91} = \left(-\frac{1}{J_{N23}} \right) \cdot \ln \left(\frac{M_{N24} + e^{J_{N25} M_{N25}} \left(M_{N21} (1 - e^{-J_{N24} M_{N24}}) + M_{N25} (1 - e^{-J_{N25} M_{N25}}) \right)}{M_{N24} + M_{N23} e^{J_{N22} M_{N22} + J_{N21} M_{N21} + J_{N24} M_{N24} + J_{N25} M_{N25} + J_{N23} T_d}} \right) \\ J_{n91} = \frac{R_{ac} + 2R_{ont}}{L_{ac}}, J_{n92} = \frac{R_{ac} + 2R_{ont} + 4N^2 R_{ont}}{L_{ac}}, J_{n93} = \frac{R_{ac} + 4N^2 R_{ont}}{L_{ac}}, J_{n94} = \frac{R_{ac} + 4N^2 R_{ont}}{L_{ac}} \\ J_{n95} = \frac{R_{ac} + 2R_{ont} + 4N^2 R_{ont}}{L_{ac}}, M_{n91} = \frac{V_1 + 2N(V_2 + 2V_{dH})}{R_{ac} + 2R_{ont}}, M_{n92} = \frac{V_1 + 2NV_2}{R_{ac} + 2R_{ont} + 4N^2 R_{ont}} \\ M_{n93} = \frac{V_1 + 2V_{dH} + 2NV_2}{R_{ac} + 4N^2 R_{ont}}, M_{n94} = \frac{V_1 + 2V_{dH} + 2NV_2}{R_{ac} + 4N^2 R_{ont}}, M_{n95} = \frac{2NV_2 - V_1}{R_{ac} + 2R_{ont} + 4N^2 R_{ont}} \end{array} \right.$$

(14) $V_2 \rightarrow V_I$, Mode c :

$$\left\{ \begin{array}{l} \text{Condition : } 2NV_2 > V_1 \wedge -d > 2T_d f_s \wedge i_L(t_{N33}) \geq 0 \\ P_{in} = -2V_1 f_s (-Int_{p91} - Int_{p92} - Int_{p93} + Int_{p94} + Int_{p95}) \\ P_o = -2V_2 \cdot 2Nf_s (Int_{p91} + Int_{p92} + Int_{p93} + Int_{p94} + Int_{p95}) \\ \Delta t_{n91} = T_d, \Delta t_{n92} = \frac{d}{2f_s} - T_d - \Delta t_{N33}, \Delta t_{n94} = T_d, \Delta t_{n95} = \frac{1}{2f_s} \cdot \frac{d}{2f_s} - T_d \\ \Delta t_{n91} = \left(-\frac{1}{J_{N32}} \right) \cdot \ln \left(\frac{M_{N33} - M_{N34} + (M_{N31} + M_{N35}) e^{J_{N32} M_{N32} + J_{N31} M_{N31}}}{M_{N33} + M_{N32} e^{J_{N31} M_{N31} + J_{N34} M_{N34} + J_{N35} M_{N35}} + (M_{N34} - M_{N35}) e^{J_{N34} M_{N34}}} \right) \\ J_{n91} = \frac{R_{ac} + 2R_{ont}}{L_{ac}}, J_{n92} = \frac{R_{ac} + 2R_{ont} + 4N^2 R_{ont}}{L_{ac}}, J_{n93} = \frac{R_{ac} + 2R_{ont} + 4N^2 R_{ont}}{L_{ac}}, J_{n94} = \frac{R_{ac} + 4N^2 R_{ont}}{L_{ac}} \\ J_{n95} = \frac{R_{ac} + 2R_{ont} + 4N^2 R_{ont}}{L_{ac}}, M_{n91} = \frac{V_1 + 2N(V_2 + 2V_{dH})}{R_{ac} + 2R_{ont}}, M_{n92} = \frac{V_1 + 2NV_2}{R_{ac} + 2R_{ont} + 4N^2 R_{ont}} \\ M_{n93} = \frac{V_1 + 2NV_2}{R_{ac} + 2R_{ont} + 4N^2 R_{ont}}, M_{n94} = \frac{2NV_2 - (V_1 + 2V_{dH})}{R_{ac} + 4N^2 R_{ont}}, M_{n95} = \frac{2NV_2 - V_1}{R_{ac} + 2R_{ont} + 4N^2 R_{ont}} \end{array} \right.$$

(15) $V_2 \rightarrow V_I$, Mode d :

$$\left\{ \begin{array}{l} \text{Condition : } 2NV_2 < V_1 \wedge -d > 2T_d f_s \wedge i_L(t_{N20}) \geq 0 \\ P_{in} = -2V_1 f_s (-Int_{p91} - Int_{p92} + Int_{p93} + Int_{p94} + Int_{p95}) \\ P_o = -2V_2 \cdot 2Nf_s (-Int_{p91} + Int_{p92} + Int_{p93} + Int_{p94} + Int_{p95}) \\ \Delta t_{n91} = T_d, \Delta t_{n92} = \frac{d}{2f_s} - T_d, \Delta t_{n93} = T_d, \Delta t_{n95} = \frac{1}{2f_s} \cdot \frac{d}{2f_s} - T_d - \Delta t_{N24} \\ \Delta t_{n91} = \left(-\frac{1}{J_{N24}} \right) \cdot \ln \left(\frac{M_{N24} + M_{N25} e^{-J_{N21} M_{N21} + J_{N22} M_{N22} + J_{N23} M_{N23} + J_{N24} \left(\frac{1}{2f_s} T_d - \frac{d}{2f_s} T_d\right)}}{M_{N24} + M_{N25} e^{-J_{N21} M_{N21} + J_{N22} M_{N22} + J_{N23} M_{N23}} - M_{N21} (1 - e^{-J_{N21} M_{N21}}) e^{-J_{N24} \left(\frac{1}{2f_s} T_d - \frac{d}{2f_s} T_d\right)}} \right. \\ \left. - M_{N22} (1 - e^{-J_{N22} M_{N22}}) e^{-J_{N23} M_{N23}} - M_{N23} (1 - e^{-J_{N23} M_{N23}}) \right) \\ J_{n91} = \frac{R_{ac} + 2R_{ont}}{L_{ac}}, J_{n92} = \frac{R_{ac} + 2R_{ont} + 4N^2 R_{ont}}{L_{ac}}, J_{n93} = \frac{R_{ac} + 4N^2 R_{ont}}{L_{ac}}, J_{n94} = \frac{R_{ac} + 2R_{ont} + 4N^2 R_{ont}}{L_{ac}} \\ J_{n95} = \frac{R_{ac} + 2R_{ont} + 4N^2 R_{ont}}{L_{ac}}, M_{n91} = \frac{-2N(V_2 + 2V_{dH}) + V_1}{R_{ac} + 2R_{ont}}, M_{n92} = \frac{V_1 + 2NV_2}{R_{ac} + 2R_{ont} + 4N^2 R_{ont}} \\ M_{n93} = \frac{2NV_2 - (V_1 + 2V_{dH})}{R_{ac} + 4N^2 R_{ont}}, M_{n94} = \frac{2NV_2 - V_1}{R_{ac} + 2R_{ont} + 4N^2 R_{ont}}, M_{n95} = \frac{2NV_2 - V_1}{R_{ac} + 2R_{ont} + 4N^2 R_{ont}} \end{array} \right.$$

(16) $V_2 \rightarrow V_I$, Mode e :

$$\left\{ \begin{array}{l} \text{Condition : } 2NV_2 < V_1 \wedge -d > 2T_d f_s \wedge i_L(t_{N20}) < 0 \wedge i_L(t_{N22}) > 0 \\ P_{in} = -2V_1 f_s (-Int_{p91} - Int_{p92} - Int_{p93} + Int_{p94} + Int_{p95}) \\ P_o = -2V_2 \cdot 2Nf_s (Int_{p91} - Int_{p92} + Int_{p93} + Int_{p94} + Int_{p95}) \\ \Delta t_{n92} = T_d - \Delta t_{N21}, \Delta t_{n93} = \frac{d}{2f_s} - T_d, \Delta t_{n94} = T_d, \Delta t_{n95} = \frac{1}{2f_s} \cdot \frac{d}{2f_s} - T_d \\ \Delta t_{n92} = \left(-\frac{1}{J_{N21}} \right) \cdot \ln \left(\frac{M_{N21} + M_{N22} e^{-J_{N23} M_{N23} + J_{N24} M_{N24} + J_{N25} M_{N25} + J_{N26} M_{N26} + J_{N27} M_{N27}}}{M_{N21} + M_{N22} e^{-J_{N23} M_{N23} + J_{N24} M_{N24} + J_{N25} M_{N25}} + M_{N23} (1 - e^{-J_{N23} M_{N23}}) e^{-J_{N24} M_{N24} + J_{N25} M_{N25}}} \right. \\ \left. + M_{N24} (1 - e^{-J_{N24} M_{N24}}) e^{-J_{N25} M_{N25}} + M_{N25} (1 - e^{-J_{N25} M_{N25}}) \right) \\ J_{n91} = \frac{R_{ac} + 2R_{ont}}{L_{ac}}, J_{n92} = \frac{R_{ac} + 2R_{ont}}{L_{ac}}, J_{n93} = \frac{R_{ac} + 2R_{ont} + 4N^2 R_{ont}}{L_{ac}}, J_{n94} = \frac{R_{ac} + 4N^2 R_{ont}}{L_{ac}} \\ J_{n95} = \frac{R_{ac} + 2R_{ont} + 4N^2 R_{ont}}{L_{ac}}, M_{n91} = \frac{V_1 + 2N(V_2 + 2V_{dH})}{R_{ac} + 2R_{ont}}, M_{n92} = \frac{-2N(V_2 + 2V_{dH}) + V_1}{R_{ac} + 2R_{ont}} \\ M_{n93} = \frac{2NV_2 - (V_1 + 2V_{dH})}{R_{ac} + 4N^2 R_{ont}}, M_{n94} = \frac{2NV_2 - V_1}{R_{ac} + 2R_{ont} + 4N^2 R_{ont}}, M_{n95} = \frac{2NV_2 - V_1}{R_{ac} + 2R_{ont} + 4N^2 R_{ont}} \end{array} \right.$$

(17) $V_2 \rightarrow V_I$, Mode f :

$$\begin{aligned}
& \text{Condition: } 2NV_2 < V_1 \wedge -d > 2T_d f_s \wedge i_L(t_{NY1}) \leq 0 \\
& P_{in} = -2V_1 f_s (-Int_{PY1} - Int_{PY2} - Int_{PY3} + Int_{PY4} + Int_{PY5}) \\
& P_o = -2V_2 \cdot 2Nf_s (Int_{PY1} + Int_{PY2} + Int_{PY3} + Int_{PY4} + Int_{PY5}) \\
& \Delta t_{df1} = T_d, \Delta t_{df3} = \frac{-d}{2f_s} - T_d - \Delta t_{NY2}, \Delta t_{df4} = T_d, \Delta t_{df5} = \frac{1}{2f_s} - \frac{-d}{2f_s} - T_d \\
& \Delta t_{df2} = \left(-\frac{1}{J_{NY2}} \right) \cdot \ln \left(\frac{M_{NY2} + M_{NY3} e^{-\left(J_{NY1} \Delta t_{NY1} + J_{NY4} \Delta t_{NY4} + J_{NY5} \Delta t_{NY5} + J_{NY3} \left(\frac{-d}{2f_s} - T_d \right) \right)}}{M_{NY2} + M_{NY3} e^{-\left(J_{NY1} \Delta t_{NY1} + J_{NY4} \Delta t_{NY4} + J_{NY5} \Delta t_{NY5} \right)} + M_{NY4} \left(1 - e^{-J_{NY4} \Delta t_{NY4}} \right) e^{-\left(J_{NY1} \Delta t_{NY1} + J_{NY3} \Delta t_{NY3} \right)}}{+ M_{NY5} \left(1 - e^{-J_{NY5} \Delta t_{NY5}} \right) e^{-J_{NY4} \Delta t_{NY4}} - M_{NY1} \left(1 - e^{-J_{NY1} \Delta t_{NY1}} \right)} \right) \\
& J_{df1} = \frac{R_{ac} + 2R_{onff}}{L_{ac}}, J_{df2} = \frac{R_{ac} + 2R_{onff} + 4N^2 R_{onL}}{L_{ac}}, J_{df3} = \frac{R_{ac} + 2R_{onff} + 4N^2 R_{onL}}{L_{ac}}, J_{df4} = \frac{R_{ac} + 4N^2 R_{onL}}{L_{ac}} \\
& J_{df5} = \frac{R_{ac} + 2R_{onff} + 4N^2 R_{onL}}{L_{ac}}, M_{df1} = \frac{V_1 + 2N(V_2 + 2V_{dl})}{R_{ac} + 2R_{onff} + 4N^2 R_{onL}}, M_{df2} = \frac{V_1 + 2NV_2}{R_{ac} + 2R_{onff} + 4N^2 R_{onL}} \\
& M_{df3} = \frac{V_1 + 2NV_2}{R_{ac} + 2R_{onff} + 4N^2 R_{onL}}, M_{df4} = \frac{2NV_2 - (V_1 + 2V_{dl})}{R_{ac} + 4N^2 R_{onL}}, M_{df5} = \frac{2NV_2 - V_1}{R_{ac} + 2R_{onff} + 4N^2 R_{onL}}
\end{aligned}$$

(18) $V_2 \rightarrow V_I$, Mode g:

$$\begin{aligned}
& \text{Condition: } 2NV_2 \approx V_1 \wedge -d > 2T_d f_s, -d < \frac{2f_s}{J_{NB4}} \cdot \ln \left(-\frac{-M_{NB2} e^{-J_{NB3} \Delta t_{NB3} + J_{NB2} T_d - J_{NB4} \left(\frac{1}{2f_s} - T_d \right)} + M_{NB4} + i_L(t_{NB0})}{(M_{NB3} - M_{NB4} + (M_{NB2} - M_{NB3}) e^{-J_{NB3} \Delta t_{NB3}})} e^{-J_{NB4} \left(\frac{1}{2f_s} - T_d \right)} \right) \\
& P_{in} = -2V_1 f_s (-Int_{PB1} - Int_{PB3} + Int_{PB4} + Int_{PB5}) \\
& P_o = -2V_2 \cdot 2Nf_s (Int_{PB1} + Int_{PB3} + Int_{PB4} + Int_{PB5}) \\
& \Delta t_{ng2} = T_d - \Delta t_{NG1}, \Delta t_{ng3} = \frac{-d}{2f_s} - T_d, \Delta t_{ng4} = T_d, \Delta t_{ng5} = \frac{1}{2f_s} - \frac{-d}{2f_s} - T_d \\
& \Delta t_{ng1} = \left(-\frac{1}{J_{NG1}} \right) \cdot \ln \left(\frac{M_{NG1}}{M_{NG1} + M_{NG3} \left(1 - e^{-J_{NG2} \Delta t_{NG2}} \right) e^{-\left(J_{NG4} \Delta t_{NG4} + J_{NG5} \Delta t_{NG5} \right)}}{+ M_{NG4} e^{-J_{NG2} \Delta t_{NG2}} \left(1 - e^{-J_{NG2} \Delta t_{NG2}} \right) + M_{NG5} \left(1 - e^{-J_{NG5} \Delta t_{NG5}} \right)} \right) \\
& J_{ng1} = \frac{R_{ac} + 2R_{onff}}{L_{ac}}, J_{ng2} = \text{Not Exist}, J_{ng3} = \frac{R_{ac} + 2R_{onff} + 4N^2 R_{onL}}{L_{ac}}, J_{ng4} = \frac{R_{ac} + 4N^2 R_{onL}}{L_{ac}} \\
& J_{ng5} = \frac{R_{ac} + 2R_{onff} + 4N^2 R_{onL}}{L_{ac}}, M_{ng1} = \frac{V_1 + 2N(V_2 + 2V_{dl})}{R_{ac} + 2R_{onff}}, M_{ng2} = \text{Not Exist} \\
& M_{ng3} = \frac{V_1 + 2NV_2}{R_{ac} + 2R_{onff} + 4N^2 R_{onL}}, M_{ng4} = \frac{2NV_2 - (V_1 + 2V_{dl})}{R_{ac} + 4N^2 R_{onL}}, M_{ng5} = \frac{2NV_2 - V_1}{R_{ac} + 2R_{onff} + 4N^2 R_{onL}}
\end{aligned}$$

(19) $V_2 \rightarrow V_I$, Mode h:

$$\begin{aligned}
& \text{Condition: } 2NV_2 \approx V_1 \wedge -d > 2T_d f_s, -d = \frac{2f_s}{J_{NB4}} \cdot \ln \left(-\frac{-M_{NB2} e^{-J_{NB3} \Delta t_{NB3} + J_{NB2} T_d - J_{NB4} \left(\frac{1}{2f_s} - T_d \right)} + M_{NB4} + i_L(t_{NB0})}{(M_{NB3} - M_{NB4} + (M_{NB2} - M_{NB3}) e^{-J_{NB3} \Delta t_{NB3}})} e^{-J_{NB4} \left(\frac{1}{2f_s} - T_d \right)} \right) \\
& P_{in} = -2V_1 f_s (-Int_{PB1} - Int_{PB2} + Int_{PB3} + Int_{PB4}) \\
& P_o = -2V_2 \cdot 2Nf_s (Int_{PB1} + Int_{PB2} + Int_{PB3} + Int_{PB4}) \\
& \Delta t_{nh1} = T_d, \Delta t_{nh2} = \frac{-d}{2f_s} - T_d, \Delta t_{nh3} = T_d, \Delta t_{nh4} = \frac{1}{2f_s} - \frac{-d}{2f_s} - T_d, \Delta t_{nh5} = 0 \\
& J_{nh1} = \frac{R_{ac} + 2R_{onff}}{L_{ac}}, J_{nh2} = \frac{R_{ac} + 2R_{onff} + 4N^2 R_{onL}}{L_{ac}}, J_{nh3} = \frac{R_{ac} + 4N^2 R_{onL}}{L_{ac}}, J_{nh4} = \frac{R_{ac} + 2R_{onff} + 4N^2 R_{onL}}{L_{ac}} \\
& J_{nh5} = \text{Not Exist}, M_{nh1} = \frac{V_1 + 2N(V_2 + 2V_{dl})}{R_{ac} + 2R_{onff}}, M_{nh2} = \frac{V_1 + 2NV_2}{R_{ac} + 2R_{onff} + 4N^2 R_{onL}} \\
& M_{nh3} = \frac{2NV_2 - (V_1 + 2V_{dl})}{R_{ac} + 4N^2 R_{onL}}, M_{nh4} = \frac{2NV_2 - V_1}{R_{ac} + 2R_{onff} + 4N^2 R_{onL}}, M_{nh5} = \text{Not Exist}
\end{aligned}$$

(20) $V_2 \rightarrow V_I$, Mode i:

$$\begin{aligned}
& \text{Condition: } 2NV_2 \approx V_1, -d > \frac{2f_s}{J_{NB4}} \cdot \ln \left(-\frac{-M_{NB2} e^{-J_{NB3} \Delta t_{NB3} + J_{NB2} T_d - J_{NB4} \left(\frac{1}{2f_s} - T_d \right)} + M_{NB4} + i_L(t_{NB0})}{(M_{NB3} - M_{NB4} + (M_{NB2} - M_{NB3}) e^{-J_{NB3} \Delta t_{NB3}})} e^{-J_{NB4} \left(\frac{1}{2f_s} - T_d \right)} \right) \\
& P_{in} = -2V_1 f_s (-Int_{PB1} - Int_{PB2} - Int_{PB3} + Int_{PB4} + Int_{PB5}) \\
& P_o = -2V_2 \cdot 2Nf_s (Int_{PB1} + Int_{PB2} + Int_{PB3} + Int_{PB4} + Int_{PB5}) \\
& \Delta t_{ni1} = T_d, \Delta t_{ni3} = \frac{-d}{2f_s} - T_d - \Delta t_{NI2}, \Delta t_{ni4} = T_d, \Delta t_{ni5} = \frac{1}{2f_s} - \frac{-d}{2f_s} - T_d \\
& \Delta t_{ni2} = \left(-\frac{1}{J_{NI2}} \right) \cdot \ln \left(\frac{M_{NI2} + M_{NI3} e^{-\left(J_{NI1} \Delta t_{NI1} + J_{NI4} \Delta t_{NI4} + J_{NI5} \Delta t_{NI5} + J_{NI3} \left(\frac{-d}{2f_s} - T_d \right) \right)}}{M_{NI2} + M_{NI3} e^{-\left(J_{NI1} \Delta t_{NI1} + J_{NI4} \Delta t_{NI4} + J_{NI5} \Delta t_{NI5} \right)} + M_{NI4} \left(1 - e^{-J_{NI4} \Delta t_{NI4}} \right) e^{-\left(J_{NI1} \Delta t_{NI1} + J_{NI3} \Delta t_{NI3} \right)}}{+ M_{NI5} \left(1 - e^{-J_{NI5} \Delta t_{NI5}} \right) e^{-J_{NI4} \Delta t_{NI4}} - M_{NI1} \left(1 - e^{-J_{NI1} \Delta t_{NI1}} \right)} \right) \\
& J_{ni1} = \frac{R_{ac} + 2R_{onff}}{L_{ac}}, J_{ni2} = \frac{R_{ac} + 2R_{onff} + 4N^2 R_{onL}}{L_{ac}}, J_{ni3} = \frac{R_{ac} + 2R_{onff} + 4N^2 R_{onL}}{L_{ac}} \\
& J_{ni4} = \frac{R_{ac} + 4N^2 R_{onL}}{L_{ac}}, J_{ni5} = \frac{R_{ac} + 2R_{onff} + 4N^2 R_{onL}}{L_{ac}}, M_{ni1} = \frac{V_1 + 2N(V_2 + 2V_{dl})}{R_{ac} + 2R_{onff}} \\
& M_{ni2} = \frac{V_1 + 2NV_2}{R_{ac} + 2R_{onff} + 4N^2 R_{onL}}, M_{ni3} = \frac{V_1 + 2NV_2}{R_{ac} + 2R_{onff} + 4N^2 R_{onL}} \\
& M_{ni4} = \frac{2NV_2 - (V_1 + 2V_{dl})}{R_{ac} + 4N^2 R_{onL}}, M_{ni5} = \frac{2NV_2 - V_1}{R_{ac} + 2R_{onff} + 4N^2 R_{onL}}
\end{aligned}$$